

Photometry of 10 Million Stars from the First Two Years of TESS Full Frame Images - Part I

Chelsea X. Huang,^{1,*} Andrew Vanderburg,² Andras Pál,¹ Lizhou Sha,^{1,2} Liang Yu,¹ Willie Fong,¹ Michael Fausnaugh,¹
Avi Shporer,¹ Natalia Guerrero,¹ Roland Vanderspek,¹ and George Ricker¹

¹*Kavli Institute for Astrophysics and Space Research, MIT*

²*Department of Astronomy, University of Wisconsin-Madison*

(Revised November 11, 2020)

ABSTRACT

The Transiting Exoplanet Survey Satellite (TESS) is the first high-precision full-sky photometric survey in space. We extracted light curves from a magnitude limited set of stars and other stationary luminous objects from the TESS Full Frame Images (FFIs) using the MIT Quick Look Pipeline (QLP). Here, we describe the techniques used to create light curves.

Keywords: TESS — survey — pipeline

INTRODUCTION

NASA’s Transiting Exoplanet Survey Satellite (TESS) mission (Ricker et al. 2015) launched on 2018 April 18, and began science operations on 2018 July 25. TESS uses four identical cameras to observe stars over a total $24^\circ \times 96^\circ$ field of view. Like *Kepler*, TESS observes stars in so-called “postage stamps,” or small subimages from the TESS cameras centered on particularly bright or important stars. However, TESS also saves and downloads images from its entire field of view every 30 minutes. These full frame images (or FFIs) greatly increase the mission’s discovery space (with some simulations projecting tens of thousands of planet discoveries from the FFIs (Barclay et al. 2018; Huang et al. 2018b)), but also substantially increase data processing requirements.

Before TESS’s launch, sophisticated and highly successful software tools were developed to analyze data from space missions like CoRoT (Auvergne et al. 2009) and Kepler (Jenkins et al. 2010). However, because none of these missions downloaded continuous FFIs, the architectures of these pipelines are difficult to adapt to a mission like TESS. In the meantime, unhindered by data downlink rates, ground-based transit surveys like HAT (Bakos et al. 2007, 2013), WASP (Pollacco et al. 2006), and KELT (Pepper et al. 2007, 2012) have been extracting light curves and searching for planets from full frame data for many years. These pipelines (e.g. Collier Cameron et al. 2009; Pál 2009, , etc.) are well suited for analyzing large volumes of wide field images.

Here, we present TESS FFI photometry technique by the MIT Quick Look Pipeline (QLP). The QLP, whose architecture includes heritage from both ground-based photometric surveys and methods developed for analysis of space-based photometry, was built to rapidly process TESS data as soon as it is beamed to Earth. The QLP has already been used to identify and alert planet candidates throughout the entire TESS Primary Mission, leading to the discovery of more than 1000 planetary candidates (Guerrero et al. 2020, *submitted to ApJS*), dozens of which have already been confirmed (e.g. Huang et al. 2018; Vanderspek et al. 2019; Armstrong et al. 2020). A subsequent article (Part II) will describe the light curve products from the TESS Primary mission.

LIGHT CURVE EXTRACTION

We extract light curves for all stars in the TESS Input Catalog (TIC, Stassun et al. 2018, 2019) with TESS magnitude brighter than 13.5 observed in the TESS Primary mission (UT 2018 July 25 - UT 2020 July 04). Figure 1 shows the

Corresponding author: Chelsea X. Huang
xuhuang@mit.edu

* Torres Postdoctoral Fellow

sky locations of stars with QLP light curves. We also added in stars with proper motion larger than 200 mas yr^{-1} and brightness between TESS Magnitude 13.5 and 15.

Our procedure is as follows:

1. We process the TESS FFIs using the TICA software (Fausnaugh et al., in prep.). The TICA software carries out correction of various instrumental effects described in [Vanderspek et al. \(2019\)](#).
2. We perform a global background subtraction using nebuliser ([Irwin 1985](#)). Because TESS orbits the Earth, its cameras experience significant levels of scattered background light. Nebuliser removes much of the large-scale (>20 pixels) scattered background features in the images.
3. We then determine an astrometric solution for each image following [Huang et al. \(2015\)](#) by relating the measured centroids of bright sources ($8 < T < 10$) to their coordinates in the TIC. This astrometric solution is then used to obtain the precise position of all catalog sources in the images. The typical astrometric precision for each frame is better than 0.1 pixel ($2''1$).
4. A reference image is constructed with the median combination of 40 good quality images within each TESS orbit (images with minimal scattered light, as well as good pointing stability). We compute difference images for each frame by directly subtracting the reference frame from each individual frames.
5. We measure the differential source brightness from the difference images by summing the flux within a series of 5 circular apertures (radii of 1.75, 2.5, 3.0, 3.5 and 8.0 pixels) centered on these positions.
6. We perform a second step of background subtraction. Nebuliser effectively removes large background variations, but leaves in some small-scale features. We therefore estimate the background levels in the difference images at the position of each source by calculating the median pixel values (with iterative outlier rejection) within annuli around the sources. The background annuli have inner radius and width of 4.0/3.0, 4.0/3.0, 4.0/3.0, 5.0/4.0 and 10.0/5.0 pixels, respectively. We subtract this background estimate from the difference fluxes for each source.
7. We convert the measured difference fluxes into absolute fluxes by adding the expected flux from each source based on the TESS magnitude estimates from the TIC and the instrument zeropoint magnitude ([Vanderspek et al. 2018](#)). This is equivalent to deblending the flux time series assuming the variations observed are from the target star.
8. The time series for each light curve is corrected to the Solar System barycentric reference frame from the TESS spacecraft reference frame following [Eastman et al. \(2010\)](#) using the coordinates of the target star at Epoch J2000, and TESS orbits vectors from JPL horizons¹.

ACKNOWLEDGMENTS

We thank the entire TESS Mission team for years of effort to make this work possible. This paper includes data collected by the TESS mission, which are publicly available from the Mikulski Archive for Space Telescopes (MAST). Funding for the TESS mission is provided by NASA's Science Mission directorate. CXH acknowledges support from the MIT Kavli Institute as a Torres postdoctoral fellow.

Software: nebuliser ([Irwin 1985](#)), FITSH ([Pál 2012](#)), Golang ([Meyerson 2014](#)), Astropy ([Astropy Collaboration et al. 2013](#); [Price-Whelan et al. 2018](#))

REFERENCES

- Astropy Collaboration, et al. 2013, A&A, 558, A33,
doi: [10.1051/0004-6361/201322068](https://doi.org/10.1051/0004-6361/201322068)
- Armstrong, D. J., et al. 2020, Nature, 583, 39,
doi: [10.1038/s41586-020-2421-7](https://doi.org/10.1038/s41586-020-2421-7)

¹ <https://ssd.jpl.nasa.gov/horizons.cgi>

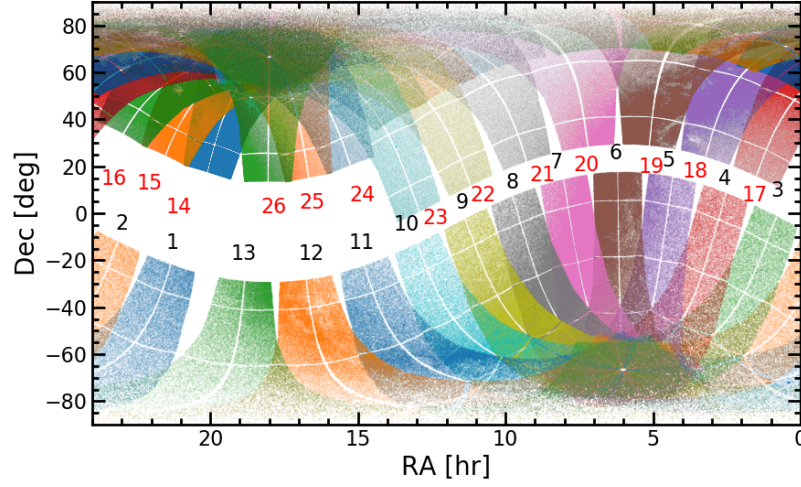


Figure 1. An illustration of all the stars for which we extracted photometry from the TESS Primary Mission FFIs in equatorial coordinates.

- Auvergne, M., et al. 2009, *A&A*, 506, 411,
doi: [10.1051/0004-6361/200810860](https://doi.org/10.1051/0004-6361/200810860)
- Bakos, G. Á., et al. 2007, *ApJ*, 656, 552,
doi: [10.1086/509874](https://doi.org/10.1086/509874)
- Bakos, G. Á., et al. 2013, *PASP*, 125, 154,
doi: [10.1086/669529](https://doi.org/10.1086/669529)
- Collier Cameron, A., et al. 2009, in *IAU Symposium*, Vol. 253, *Transiting Planets*, ed. F. Pont, D. Sasselov, & M. J. Holman, 29–35
- Barclay, T., et al. 2018, *ApJS*, 239, 2,
doi: [10.3847/1538-4365/aac3e9](https://doi.org/10.3847/1538-4365/aac3e9)
- Eastman, J., Siverd, R., & Gaudi, B. S. 2010, *PASP*, 122, 935, doi: [10.1086/655938](https://doi.org/10.1086/655938)
- Huang, C. X., et al. 2015, *MNRAS*, 454, 4159,
doi: [10.1093/mnras/stv2257](https://doi.org/10.1093/mnras/stv2257)
- Huang, C. X., et al. 2018, *ApJ*, 868, L39,
doi: [10.3847/2041-8213/aaef91](https://doi.org/10.3847/2041-8213/aaef91)
- Huang, C. X., et al. 2018b, *arXiv e-prints*,
arXiv:1807.11129. <https://arxiv.org/abs/1807.11129>
- Irwin, M. J. 1985, *MNRAS*, 214, 575,
doi: [10.1093/mnras/214.4.575](https://doi.org/10.1093/mnras/214.4.575)
- Jenkins, J. M., et al. 2010, *ApJL*, 713, L87,
doi: [10.1088/2041-8205/713/2/L87](https://doi.org/10.1088/2041-8205/713/2/L87)
- Meyerson, J. 2014, *IEEE software*, 31, 104
- Pál, A. 2009, PhD thesis, Department of Astronomy, Eötvös Loránd University
- Pál, A. 2012, *MNRAS*, 421, 1825,
doi: [10.1111/j.1365-2966.2011.19813.x](https://doi.org/10.1111/j.1365-2966.2011.19813.x)
- Pepper, J., et al. 2007, *PASP*, 119, 923, doi: [10.1086/521836](https://doi.org/10.1086/521836)
- Pepper, J., et al. 2012, *PASP*, 124, 230, doi: [10.1086/665044](https://doi.org/10.1086/665044)
- Pollacco, D. L., et al. 2006, *PASP*, 118, 1407,
doi: [10.1086/508556](https://doi.org/10.1086/508556)
- Price-Whelan, A. M., et al. 2018, *AJ*, 156, 123,
doi: [10.3847/1538-3881/aabc4f](https://doi.org/10.3847/1538-3881/aabc4f)
- Ricker, G. R., et al. 2015, *Journal of Astronomical Telescopes, Instruments, and Systems*, 1, 014003.
doi: [10.1117/1.JATIS.1.1.014003](https://doi.org/10.1117/1.JATIS.1.1.014003)
- Stassun, K. G., et al. 2018, *AJ*, 156, 102,
doi: [10.3847/1538-3881/aad050](https://doi.org/10.3847/1538-3881/aad050)
- Stassun, K. G., et al. 2019, *AJ*, 158, 138,
doi: [10.3847/1538-3881/ab3467](https://doi.org/10.3847/1538-3881/ab3467)
- Vanderspek, R., et al. 2018, *TESS Instrument Handbook*, TESS Science Office
- Vanderspek, R., et al. 2019, *ApJL*, 871, L24,
doi: [10.3847/2041-8213/aafb7a](https://doi.org/10.3847/2041-8213/aafb7a)